Spray-Deposited Large-Area Copper Nanowire Transparent Conductive Electrodes and Their Uses for Touch Screen Applications

Hsun-Chen Chu, Yen-Chen Chang, Yow Lin, Shu-Hao Chang, Wei-Chung Chang, Guo-An Li, and Hsing-Yu Tuan*

Department of Chemical Engineering, National Tsing Hua University, 101, Section 2, Kuang-Fu Road, Hsinchu, Taiwan 30013, Republic of China

S *Supporting Information*

ABSTRACT: Large-area conducting transparent conducting electrodes (TCEs) were prepared by a fast, scalable, and low-cost spray deposition of copper nanowire (CuNW) dispersions. Thin, long, and pure copper nanowires were obtained via the seed-mediated growth in an organic solvent-based synthesis. The mean length and diameter of nanowires are, respectively, 37.7 μm and 46 nm, corresponding to a high-mean-aspect ratio of 790. These wires were spray-deposited onto a glass substrate to form a nanowire conducting network which function as a TCE. CuNW TCEs exhibit high-transparency and high-conductivity since their relatively long lengths are advantageous in lowering in the sheet resistance. For example, a 2×2 cm^2 transparent nanowire electrode exhibits transmittance of $T = 90\%$ with a sheet resistance as low as 52.7 Ω sq^{-1}. Large-area sizes (>50 cm^2) of CuNW TCEs were also prepared by the spray coating method and assembled as resistive touch screens that can be integrated with a variety of devices, including LED lighting array, a computer, electric motors, and audio electronic devices, showing the capability to make diverse sizes and functionalities of CuNW TCEs by the reported method.

KEYWORDS: *copper, nanowire, spray deposition, transparent conductive electrode, touch screen, large-area*

1. INTRODUCTION

With the prosperity of optoelectronic industry, the role of transparent conductive electrode (TCE) becomes more and more indispensable. For example, TCE has been used on light-emitting diodes (OLEDs), solar cells, and touch screens.[1-3] Especially, touch screens greatly facilitate our daily life since they can be integrated into tablet personal computers, car navigation, and smart phones.[4] Because of their light weight, simplicity, transparency, and multitouch capability, touch screens can reduce the weight of device.[4,5] A screen and buttons can be combined in the form of a touch screen, and the volume of a device can be effectively conserved. Therefore, a touch screen has gradually substituted for a button in the form of acoustic wave (SAW),[6] infrared,[7] capacitive,[8] or resistive[9] types. Resistive touch screens play a critical role in the global market of touch screens because of their simple structure, low-power consumption, high-resolution, and low-prices.[10] In the structure of resistive touch screens, two TCEs made by transparent and insulating substrates (glass or acrylic panel) are coated with conductive layers. The two conductive layers are oppositely placed and separated with invisible spacers.[9,10]

For the past decades, indium-doped tin oxide (ITO) had always been the dominant material used for the TCE market due to its excellent characters regarding both transmittance (90%) and conductance (10 Ω sq^{-1}). However, the massive consumption of ITO leads to price inflation of the scarce element indium. Moreover, the ceramic nature and high-reflection characteristic of ITO limit its application in flexible substrates and near-IR optoelectronic devices. To solve these problems, it is inevitable to find other materials to substitute for ITO. Recently, various materials, including conducting polymers,[11,12] carbon nanotubes (CNTs),[13-16] graphene,[17-19] and metal nanowires[20-26] were used as ITO alternatives. Among these materials, the sheet resistance of solution-processed CNT and graphene is still too high to reach the minimum standards required by industry for TCEs ($T > 90\%$ and Rs < 100 Ω sq^{-1}).[27,28] On the other hand, random distribution of metal nanowires exhibits promising results. Nanowire TCEs can be made via scalable coating methods, such as spray coating or roll-to-roll coating. The performance of silver nanowires (AgNWs)[29] is comparable to ITO, superior to all the other ITO-alternative materials. Nevertheless, the price of AgNWs is also relatively high owing to its low-abundance.

Compared with silver, copper is 1000 times more abundant and 100 times less expensive.[30] Moreover, the conductance of copper ($\sigma = 5.96 \times 10^7$ S/m) is only slightly lower than silver ($\sigma = 6.3 \times 10^7$ S/m), ranking the second among all of the metals. Wiley et al. prepared copper nanowire (CuNW) TCE
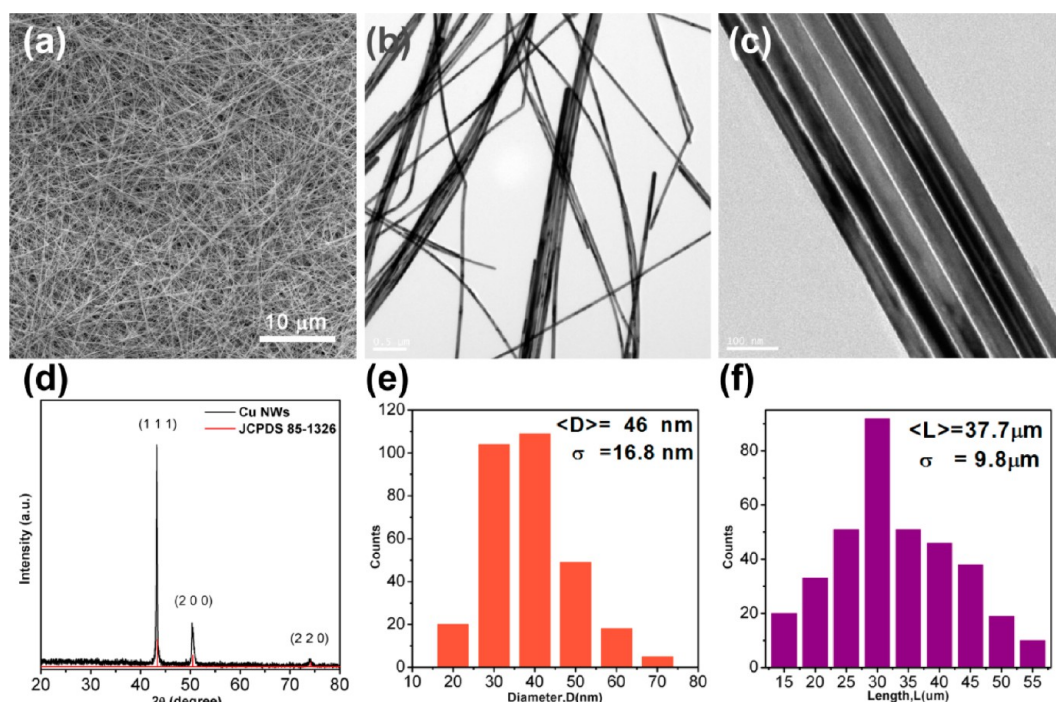
Figure 1. (a) SEM image of CuNWs. (b, c) TEM images of CuNWs. (d) XRD pattern of the CuNWs on glass substrate. Histograms of the (e) diameter and (f) length of CuNWs.

with filtration method with transmittance (T = 67%) and sheet resistance (Rs = 61 Ω sq^{-1}).[31] The quality-improved CuNW TCE with transmittance T = 90% (Rs = 186 Ω sq^{-1})[20] processed through the mayer rod coating method was reported later. Dieqing Zhang and co-workers used a nonaqueous method to synthesize ultralong single crystalline CuNWs and make TCEs by the vacuum filtration method to obtain performance of Rs = 90 Ω sq^{-1} at T = 90%.[32] Yang's group synthesized ultrathin CuNWs (d = 17.5 nm) by using tris(trimethylsilyl)silane as a mild reducing reagent for TCE applications with performance in transmittance and 34.8 Ω sq^{-1} in sheet resistance.[33] Cu is oxidized easily when they are exposed to air. Rathmell et al. reported the method of Ni-coated CuNWs synthesis and its application in TCE. Owing to the protection of the Ni layer, the oxidation of CuNWs was effectively avoided, and the sheet resistance of CuNW TCE remains almost constant after 30 days.[34] In 2015, Sun's group reported the facile mothed for the synthesis of Cu–Ni and Cu–Ag bimetallic nanowires. With the protection of the Ni and Ag cover layer, CuNWs have the ability to resist the thermal oxidation and moisture corrosion.[35] Besides, graphene is a good protecting material for CuNWs; a CuNW–graphene core–shell structure was published by Ahn et al. in 2015.[36] The TCE made by these nanowires shows high-optical transmittance (T = 89.3%, Rs = 53.8 Ω sq^{-1}) and outstanding oxidation stabilty (the Rs increases less than 9% after 30 days). Reduced graphene oxide (RGO)/CuNWs hybrid films were reported by Kholmanov et al., and the RGO layer deposited on CuNW network not only prevents oxidation of CuNW film but also improves electronic conductivity and substrate adhesion.[37] In addition, transparent metal oxide shells on surface of CuNWs such as Zn, In, or Sn also have the ability to protect CuNWs from oxidation without losing the transmittance of film.[38] Recently, Im et al. reported a glass-fabric reinforced CuNW-GFR Hybrimer film. The embedded CuNW structure exhibits

high-oxidation resistance; under 80 °C annealing, the sheet resistance of film shows no obvious change after 14 days.[39]

For industry applications of deposition of transparent conductive layers, a low-cost, simple, low-operating temperature, and scalable method is necessary. Spray deposition is an appropriate way to conform to the above requirements. It is easy to control the transparency and the electric conductivity of TCEs by adjusting the spraying frequency and the concentration of conducting materials. Several studies of fabricated TCEs made by different nanomaterials, including CNTs,[14,40,41] graphene,[42,43] and AgNWs[21,44] using a spray coating have been reported.

Herein, thin, long, and well-dispersed CuNWs with gram scale throughput were obtained via the seed-mediated growth in an organic solvent-based synthesis.[45] The CuNW TCEs were prepared by a simple, facile, and low-cost spray coating method. Properties of CuNW TCEs such as transmittance and sheet resistance were characterized in detail. Spray-deposited CuNW TCEs exhibit high-performance (e.g., Rs = 52.7 Ω sq^{-1} at T = 90%) and uniform transmittance in the visible and NIR region. Moreover, two different large-area sizes of CuNW TCEs (6.5 × 10 cm^2 and 6 × 25 cm^2) were prepared by spray deposition and assembled as a resistive touch screen with high-transparency and low-sheet resistance which can be applied on switching different devices.

2. RESULTS AND DISCUSSION

2-1. Synthesis of CuNWs. CuNWs were synthesized by the amine reduction method reported previously[45,46] with modified synthetic parameters. During the reaction, first, a Cu$^+$-oleylamine complex formed when solution was heated to 110 °C. After elevating the temperature, Cu$^+$ ions become Cu^{2+} and Cu^0 by means of a disproportional reaction, and 5-fold twinned CuNWs were generated.[45,46] In order to acquire longer CuNWs, the reaction condition was optimized by investigating

the synthesis of CuNWs in various reaction temperatures (see Figure S1 in Supporting Information). We found that synthesis carried out at 260 °C can produce the best quality of CuNWs, as shown in the SEM image (Figure 1a). The CuNWs afforded by the reaction condition were nearly 4 times longer than those from Han's report. The TEM images of CuNWs were shown in Figure 1b,c; the CuNWs were deposited on a holey carbon-coated copper grid. In Figure 1b, the diameter of CuNWs is uniform, and there are very few impurities (nanoparticles or byproducts) existing in the products. A self-assembly phenomena was observed in the TEM image with higher magnification as shown in Figure 1c. Figure 1d shows the XRD pattern collected from the as-prepared CuNWs, and three diffraction signals can be readily indexed at $2\theta = 43.5°$, $50.7°$, and $74.48°$, which, respectively, correspond to the (111), (200), and (220) crystal planes of face-centered-cubic (fcc) copper (JCPDS 85-1326). There are no extra signals observed, indicating high-purity of CuNWs and no other crystallites observed in the product. The diameters and lengths of CuNWs were measured and illustrated in the form of histograms in Figure 1e,f. The diameters vary from 20 to 70 nm with a mean value of 46 ± 16.8 nm, and the lengths vary from 15 to 55 μm with a mean value of 37.7 ± 9.8 μm. Figure 2a shows the digital image of large-scale CuNW solution obtained from the reaction using 4.5 g CuCl and 400 mL OLA as precursor solution. After purification, more than 2 g of CuNWs was obtained in a single reaction. Figure 2b,c shows SEM images of highly dense CuNWs synthesized by the scale-up method. This approach provides a large amount of nanowire ink, which could be used for applications of large-area of CuNW TCEs. These CuNW powders that consist of CuNWs were easily untangled and dispersed in toluene by a continuous sonication because of the oleophilic OLA capping layer on the surface of CuNWs. In order to avoid the aggregation of CuNWs which could obstruct the nozzle of spray gun, keeping the concentration of CuNW dispersion under a concentration of 0.5 mg/mL is suitable for spray coating.

2-2. Electrical Conductivity and Optical Transmittance of CuNW TCEs.

Figure 3 shows the experimental setup of the spray-deposited method. Low-concentration of CuNW ink was sprayed onto the precleaned bare glass substrate. During deposition, the CuNWs curved and partially fused because of the high-kinetic energy of spraying. As a result, the contact area between CuNWs was increased. After removing the insulating ligands on the surface of CuNWs, the electrons transferred through the wire–wire junction were more efficient. The density of CuNW networks can be easily controlled by adjusting the deposition time of the spray coating process; Figure 4 shows SEM images of CuNW films with different densities on glass substrates fabricated by the simple spray coating process. To facilitate SEM analysis, we deposited Au onto the films after spray coating. The deposited masses of CuNWs per unit area (M/A) of each film were measured. As the thickness is increased, the networks become less sparse with the substrate appearing less frequently. As the film density increases, there are fewer holes in the films, which lead to more uniform electrical field distribution when used in optoelectronic devices. Lower densities of CuNWs (Figure 4a) resulted in a higher transmittance ($T = 90.4\%$) and a higher sheet resistance ($Rs = 52.7$ Ω sq^{-1}). As the density of the nanowires is increased (Figure 4d), both the transmittance ($T = 70.8\%$) and sheet resistance decreased ($Rs = 7.6$ Ω sq^{-1}).
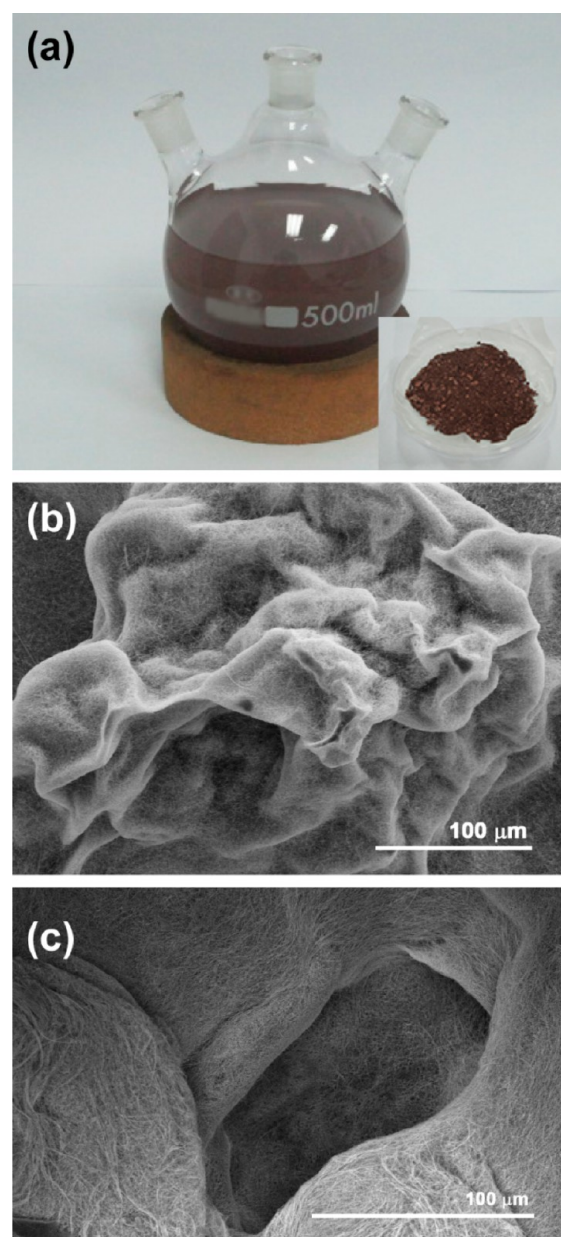

Figure 2. (a) Digital images of large-scale CuNW solution and powders. (b, c) SEM image of high-density CuNWs with different resolution magnification.

The transmittance spectra in the visible region for all films were measured (Figure 5a). There is no apparent variation in transmittance in the region between 400 and 700 nm; in other words, no particular wavelength of lights was obstructed when passing through the CuNW TCEs. A four-probe method was used to measure sheet resistance which can avoid contact resistance between probe and CuNWs. Higher transmittance of CuNWs (95.1%) resulted in a higher resistance (356.7 Ω sq^{-1}). As the amount of CuNW deposition increased, both the transmittance (61.2%) and sheet resistance (2.7 Ω sq^{-1}) dropped. The transmittance of CuNW TCEs almost maintained constant from wavelengths of 400 to 2500 nm; on the other hand, ITO is highly transparent in the visible region, but the transmittance decreases after the wavelength rises to 700 nm. Similar to ITO, the transmittance of fluorine-doped tin oxide (FTO) decrease dramatically after the wavelength rises to
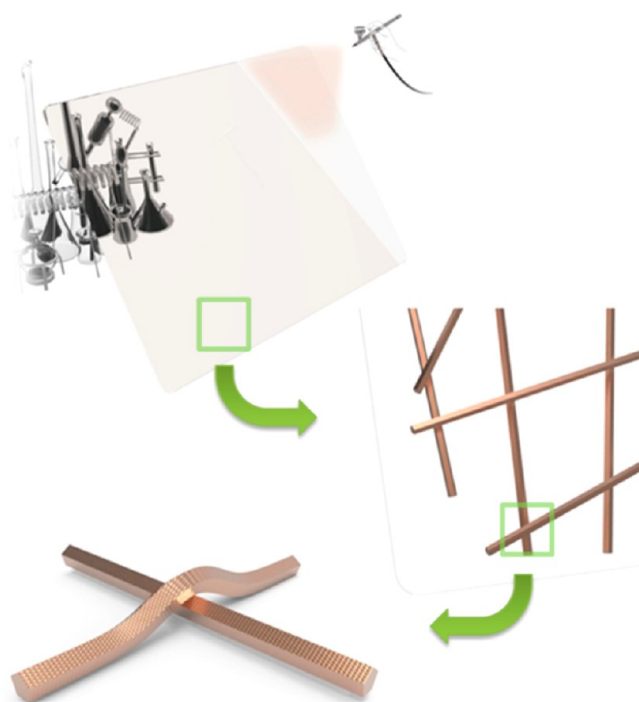
Figure 3. Experimental setup of spray-deposited method.

1000 nm. The decrease of transmittance results from ITO's and FTO's plasma resonant wavelength at about 700 and 1000 nm, respectively, which depends on the doping level,[47] as shown in Figure 5b.

The specular transmittance and the diffusive transmittance of five groups of CuNW TCEs were also measured. Specular transmittance was measured by detecting only light that comes out of the sample parallel to the incident light. The diffusive

transmittance only differed from specular transmittance in that diffusive transmittance includes all forward scattered light measured using an integrating sphere. As shown in Figure 5c, the CuNW TCEs also show higher diffusive transmittances than specular transmittances. Figure 5d shows the percentage differences between diffusive transmittances and specular transmittance corresponding to Figure 5c with values approximately ranging from 1.0 to 2.4%. TCEs with higher transmittance have smaller percentage differences. A large percentage difference leads to haze which is undesirable for display applications; however, it could be advantageous for certain devices used where light scattering is preferred, such as solar cells.[48,49] Figure 5e shows the percentage differences between diffusive transmittances and specular transmittance of different materials at specular transmittance equal to 80%. The values of FTO, ITO, CNT, and graphene are slight because of their smooth surface;[50] on the contrary, AgNW and CuNF have larger differences due to intrinsic properties and larger nanowire diameter.[22,48] The value of the CuNW TCE is 1.7% which is close to that from the previous report.[20] It should be noted that the difference is about 1% at transmittance 90%, Figure 5d, very close to the values for FTO and ITO.

The rectifying behavior was determined by using a transmission line model (TLM) measurement. As shown in Figure 6a, there is a linear $I-V$ characteristic behavior with different transmittances, which indicates that the nanowire network in the CuNW TCEs exhibits ohmic contact. The CuNW TCEs with different transmittance and conductivities were placed under air circumstance; the increasing of sheet resistance for each CuNW TCE caused from the oxidation of CuNWs was measured periodically. As shown in Figure 6b, after 38 days, electrodes with transmittance under 79.1% have negligible increase on the resistance, and electrodes with higher transmittance have little increase on the resistance. The increase may be due to the oxidation of CuNWs; the Cu_2O
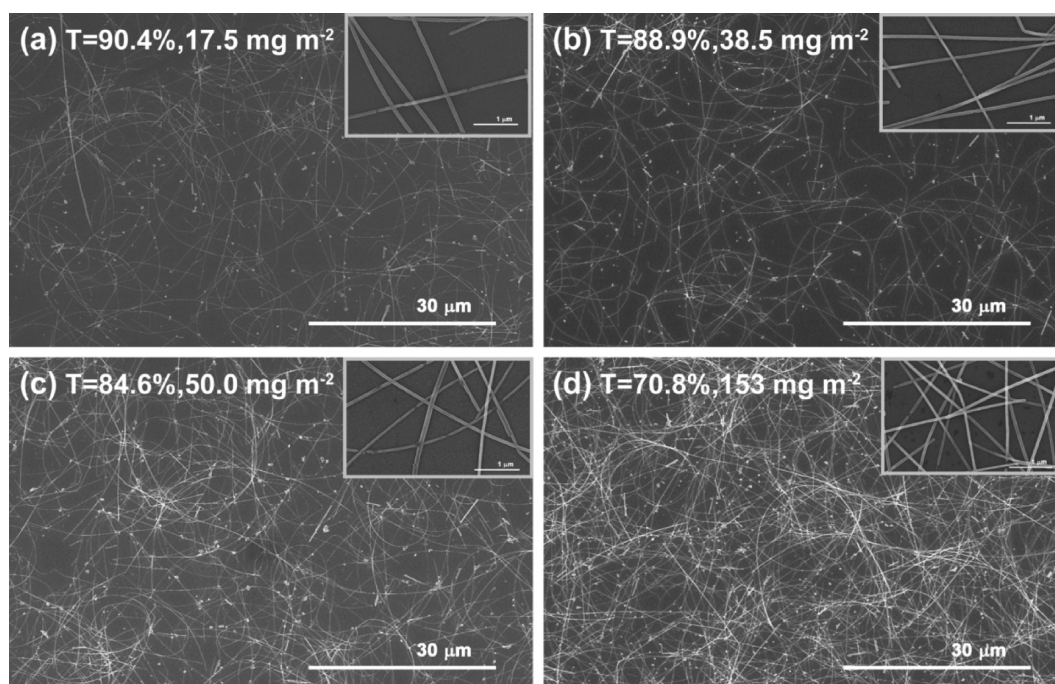

Figure 4. SEM image of CuNW films with different weight densities on glass substrates: (a) density = 17.5 mg m^{-2}, (b) density = 38.5 mg m^{-2}, (c) density = 50.0 mg m^{-2}, (d) density = 153 mg m^{-2}.
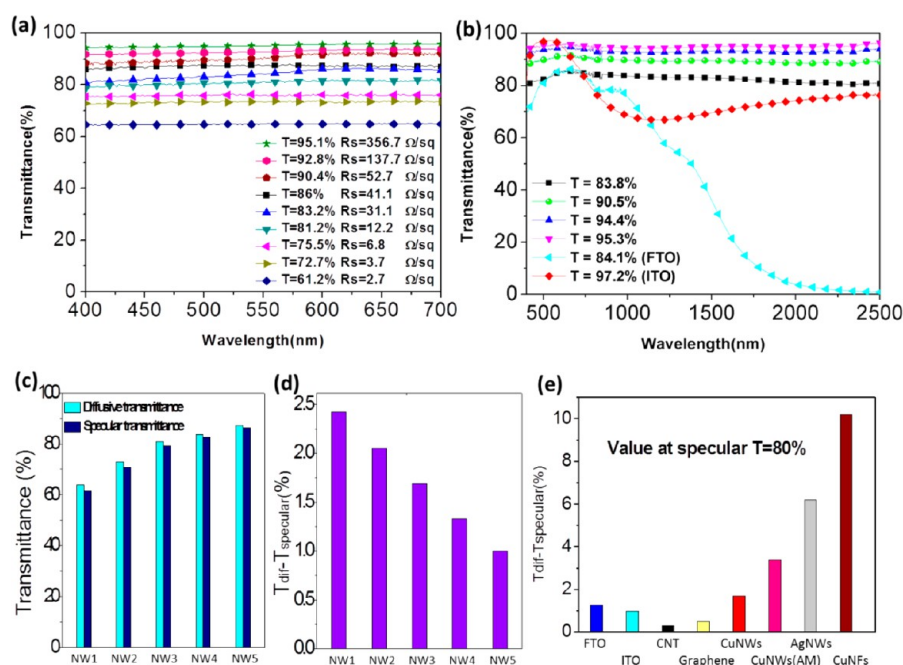
Figure 5. (a) Transmittance spectra of CuNW TCE in the visible region measured with a UV−vis spectrometer. (b) Transmittance spectra in the near-IR region (from 400 to 2500 nm) measured with a UV−vis spectrometer. (c) The diffusive transmittance and specular transmittance of CuNW TCE measured using an integrating sphere. (d) The differences of diffusive transmittances and specular transmittance correspond to part c. (e) The differences of diffusive transmittances and specular transmittance of different materials at specular transmittance 80% which were discussed in previous publication.
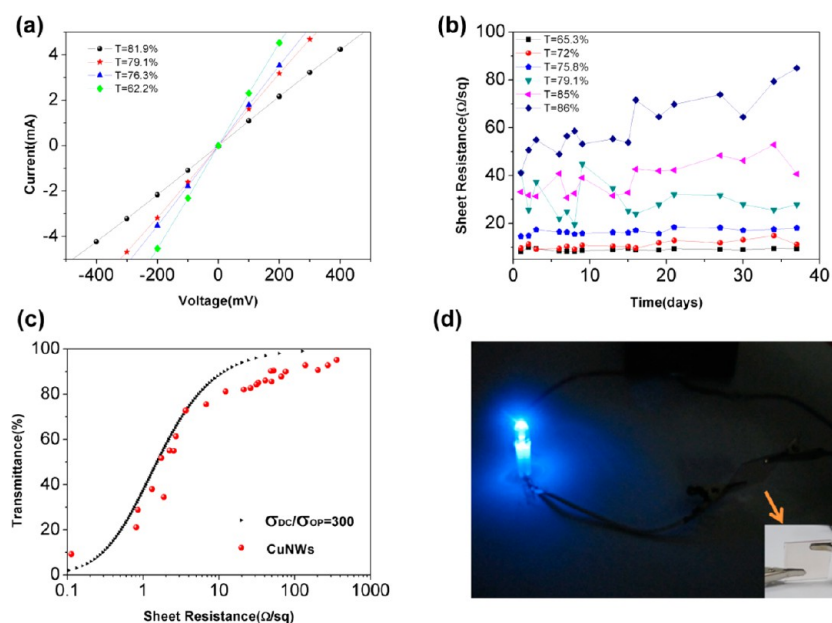

Figure 6. (a) Linear *IV* characteristics of TCEs with different transmittance. (b) CuNW TCEs with different transmittance and conductivities under air circumstance. (c) Transmittance (550 nm) plotted as a function of film sheet resistance for the films studied in this work. (d) A 2 cm × 2 cm CuNW TCE was connected with a battery and a blue light LED to form a circuit, and the LED was turned on successfully.

formed and then changed into CuO gradually when the CuNW TCEs were exposed to an ambient atmosphere.[51,52] Compared to high-transmittance electrodes, lower transmittance electrodes exhibited lower sheet resistance increasing after exposure to the air for a long time. There is no significant increase in the sheet resistance of these low-transmittance CuNW TCEs (T = 75.8%, 72%, and 65.3%), indicating the good stability of these films in air. We suspect that it is caused by the large amount of CuNW on the substrates: the upper CuNWs were oxidized

primarily and the lower CuNWs were protected by them. Therefore, more unoxidized CuNWs remained on the substrates that led to the oxidation stability.

The utility of transparent conductive electrode is largely governed by two critical parameters: the sheet resistance and transmittance. These two parameters are governed by the dc conductivity (σ_{DC}) and optical conductivity (σ_{Op}). An expression between sheet resistance, optical transmittance, σ_{DC}, and σ_{Op} is given by the following formula (eq 1)[40] which is

valid for thin metal films and has previously been shown to accurately describe films of both silver nanowires[23] and carbon nanotubes.[14]

$$T(\lambda) = \left(1 + \frac{188.5}{R_s} \frac{\sigma_{Op}(\lambda)}{\sigma_{DC}}\right)^{-2} \tag{1}$$

The best performance of CuNW TCEs in this work could fit the value σ_{DC}/σ_{Op} = 300 (Figure 6c). Previous works have demonstrated that the maximum σ_{DC}/σ_{Op} values of AgNWs and CNT are 500[23] and 25,[14] and the maximum σ_{DC}/σ_{Op} value of AgNWs by spray coating is 415.[21] The value of CuNW electrodes is much higher than CNT and slightly inferior to AgNWs. In Figure 6d, the 2 × 2 cm^2 CuNW thin film was put into a circuit with a battery pack and an LED. As can be seen, electron current can transfer through the CuNW thin film, and the LED bulb was lighted. Figure 7 shows the comparison with
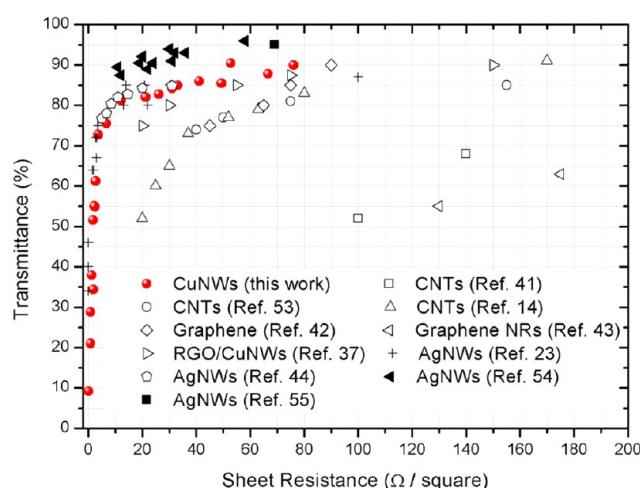

Figure 7. Sheet resistance (Ohm/square) vs transmittance (%) of TCEs made of various kinds of nanomaterials using spray-deposited methods.

previous publications which use a spray-deposited method to make TCEs; the performance of CuNW TCEs in this work outperform the CNTs electrodes[14,41,53] and graphene electrodes,[42,43] being slightly better than the RGO/CuNWs which Kholmanov reported,[37] very close to AgNWs.[23,44,54,55]

2-3. Fabrication of Large-Area CuNW TCEs and Assembled as Touch Screen Devices. As discussed above, we have successfully demonstrated the electric conductivity of 2 × 2 cm^2 CuNW TCEs. For further application testing, two pieces of large-area CuNW TCEs with approximately 83% in transmittance were combined to manufacture a resistive touch screen. Figure 8a shows the structural diagram of a 6.5 × 10 cm^2 touch screen made by CuNW TCEs. A glass/CuNWs/spacer/CuNWs/glass structure provided a high-optical transmitting area and a controllable current path. While the touch screen was pressed, the upper and bottom CuNW films were in contact to form a circuit. Electrons can pass through the touch screen through the connected CuNW films. After removal of the pressing force, the glass substrate and CuNW film restored, and the circuit was broken down. Therefore, we can easily control the devices by pressing the CuNW touch screen. The 6.5 × 10 cm^2 CuNW touch screen was examined in lighting the LED, turning on the computer, starting the electric fan, and turning on the speaker, as shown in Figure 8b. Four different

devices were separately connected to one part of the touch screen and a power source. After pressing the upper CuNW TCE, a contact occurred between two CuNW TCEs, a circuit formed simultaneously, and the devices were propelled. As shown in video S1, each part of the CuNW touch screen can individually let electrons pass and turn on devices without disturbing each other. We also demonstrate large-area TCEs by using this method. A large-area CuNW touch screen consists of two TCEs with area size of 6 × 25 cm^2 were made and tested for their applications as a touch screen. The CuNW touch screen was connected with a 3 V coin cell primary lithium battery and an LED array which was composed of 126 green LEDs and a bread board. As shown in Figure 8c and video S2, while we pressed several places on the touch screen, the LED array could be lit up. The result indicates that the circuit formed at any contacting position of the two CuNW TCEs. The current intensity in this system was measured to be 880 mA, showing that the CuNW TCE can tolerate intensive current. Large-area CuNW touch screens can form a circuit, transfer electrons, and turn on diversified devices by pressing different places on the touch screen, which means that they can be applied in electronic products requiring large-area touch screens such as a global positioning system (GPS) and an automated teller machine (ATM).

3. CONCLUSION

In summary, by using a spray-deposited method, we have successfully manufactured CuNW TCEs with high-transparency and high-conductivity. The transmittance of CuNW TCEs, the morphology of CuNW conducting network on substrate, and the electric conductivity of CuNW TCEs can be easily tuned by controlling the spraying conditions. After adjusting the transmittance of CuNW TCEs to T = 90%, the sheet resistance is 52.7 Ω sq^{-1}, very close to the performance of AgNWs. In the visible region, CuNW TCEs have the ability to transfer almost all the wavelengths of light; no particular wavelength was obstructed. In comparison to ITO, CuNW TCEs also exhibit excellent light penetration in NIR region. Large-area CuNW TCEs fabricated by spray deposition were accomplished. The CuNW TCEs were also assembled as resistive touch screens to turn on different devices, indicating that touch screens made by CuNW TCEs have the potential to be applied in optoelectronic devices with various sizes.

4. EXPERIMENTAL METHODS

4-1. Chemicals. Copper chloride (CuCl, 99.9%), oleylamine (70%), and toluene ($C_6H_5CH_3$, 99.9%) were purchased from Sigma–Aldrich and used without further purification. Copper grids were purchased from Electron Microscope Sciences. All the experiments were carried out under argon flow by using a Schlenk line.

4-2. Synthesis of Oleylamine-Coated Copper Nanowires. Typically, copper chloride (0.3 g) and oleylamine (30 mL) were added into a three-neck flask under stirring. Until all of the CuCl dissolved, the solution was heated to 110 °C under argon flow to remove the water and oxygen. After 30 min of heating, the color of solution changed from green to yellow. Afterword, the solution was heated to 260 °C and reacted for 30 min under argon protection. The color of the solution changed from pale yellow to reddish within a minute. After the reaction, the obtained copper nanowires were purified by centrifugation at 8000 rpm 5 min until the upper suspension was completely clear (three to four rounds). The CuNWs were then stored in a vial under argon conditions to prevent oxidation.

4-3. Fabrication of CuNW TCEs and Touch Screens. The CuNW thin films were prepared with a simple, facile, and low-cost

Figure 8. (a) Schematic diagram of the structure of CuNW touch screen (left) and concept of CuNW touch screen (right). (b) The 6.5 × 10 cm^2 CuNW touch screen fabricated by two CuNW TCEs was applied in turning on the computer, LED, electric fan, and speaker. The associated video showing the operation details is shown in video S1. (c) The 6× 25 cm^2 CuNW touch screen was applied in lighting a LED array, circuit is form by touching different places on the touch screen. The associated video showing the operation details is shown in video S2.

spray coating method. The CuNWs were dispersed in toluene with a concentration of 0.5 mg/mL and were sprayed onto the glass substrate

(2 cm × 2 cm) using an airbrush with back pressure with 20 psi. To prevent coalescence into larger droplets before drying, the glass

substrate was placed on a hot plate (110 °C) to accelerate the evaporation of toluene. Different densities of nanowires on the surface of the substrate were obtained by varying the amount of spraying. The CuNW films were not conductive before annealing in a furnace for 2 h in an atmosphere of 75% argon and 25% hydrogen at a reducing pressure to remove the oleylamine and the copper oxide on the surface of the CuNWs. After annealing, the CuNW films were stored under argon conditions for further characterization. In fabrication of the 6.5 × 10 cm^2 CuNW touch screen, first, a cross-shaped tape was covered on the glass substrate; after spraying, the tape was removed, and four CuNW TCE regions were formatted. After annealing, two CuNW TCEs made by the same procedure were combined; the CuNW side of one TCE faced the CuNW side of the other TCE. In order to avoid the contact between two CuNW TCEs, a cross-shaped transparent spacer was stuck on both of the CuNW-free regions of two TCEs. The four parts of CuNW touch screen were individually connected to four different devices (LED, computer, electric motor, and audio electronic device) and power sources such as lithium ion battery by electric wires. One side of the wires was connected to the upper CuNW TCEs, and the other head was connected to the bottom CuNW TCEs. The procedure of 6 × 25 cm^2 CuNW touch screen fabrication is similar to that for the 6.5 × 10 cm^2 CuNW touch screen; the two CuNW film were separated by a spacer layer, and the touch screen was connected to a LED lighting array and a lithium ion battery.

4-4. Characterization. SEM images were taken with HITACHI-S4700 and JEOL 7000F scanning electron microscopes. TEM images were taken with a HITACHI H-7100 transmission electron microscope. HR-TEM images and diffraction pattern were taken with a JEOL JEM-3000F electron microscope. When preparing the sample, a drop of toluene dispersion of copper nanowires was placed on carbon-coated copper grids and dried in air. Powder XRD patterns were collected on a MAC Science MXP18 diffractometer with Cu Kα radiation. The weight of glass substrates was measured with Sartosius SE2. The transmittance and sheet resistance of each CuNW electrode were measured using a UV−vis spectrometer (H-4100) with a blank substrate as the reference and a four-point probe (Keithley 2400) to avoid contact resistance between the probe and CuNW. Each data point of sheet resistance data is the average of 5 measurements.

■ ASSOCIATED CONTENT

Ⓢ Supporting Information

The Supporting Information is available free of charge on the ACS Publications website at DOI: 10.1021/acsami.6b02652.

> SEM images of CuNWs synthesized in various reaction temperatures (PDF)
>
> Demonstration of the 6.5 × 10 cm^2 CuNW touch screen (MPG)
>
> Demonstration of the 6 × 25 cm^2 CuNW touch screen (MPG)

■ AUTHOR INFORMATION

Corresponding Author

*E-mail: hytuan@che.nthu.edu.tw.

Author Contributions

H.-C.C., Y.-C.C., and Y.L. contributed equally to this work.

Notes

The authors declare no competing financial interest.

■ REFERENCES

(1) Li, L.; Yu, Z.; Hu, W.; Chang, C.-h.; Chen, Q.; Pei, Q. Efficient Flexible Phosphorescent Polymer Light-Emitting Diodes Based on Silver Nanowire-Polymer Composite Electrode. *Adv. Mater.* **2011**, 23 (46), 5563−5567.

(2) Yu, Z.; Li, L.; Zhang, Q.; Hu, W.; Pei, Q. Silver Nanowire-Polymer Composite Electrodes for Efficient Polymer Solar Cells. *Adv. Mater.* **2011**, 23 (38), 4453−4457.

(3) Lee, J.; Lee, P.; Lee, H. B.; Hong, S.; Lee, I.; Yeo, J.; Lee, S. S.; Kim, T.-S.; Lee, D.; Ko, S. H. Room-Temperature Nanosoldering of a Very Long Metal Nanowire Network by Conducting-Polymer-Assisted Joining for a Flexible Touch-Panel Application. *Adv. Funct. Mater.* **2013**, 23 (34), 4171−4176.

(4) Yeh, M.-K.; Chang, L.-Y.; Lu, M.-R.; Cheng, H.-C.; Wang, P.-H. Bending Stress Analysis of Flexible Touch Panel. *Microsyst. Technol.* **2014**, 20 (8−9), 1641−1646.

(5) Shin, Y.-H.; Cho, C.-K.; Kim, H.-K. Resistance and Transparency Tunable Ag-inserted Transparent InZnO Films for Capacitive Touch Screen Panels. *Thin Solid Films* **2013**, 548, 641−645.

(6) Adler, R.; Desmares, P. J. An Economical Touch Panel Using SAW Absorption. In *40th Annu. Symp. Freq. Control* 28−30 May 1986; pp 237−240.

(7) Zheng, W.; Wei, L.; Qing, H.; Ning, W.; Chenxi, W.; Tingfang, Y.; Chao, H.; Meng, M. Q. H. The Design of Infrared Touch Screen Based on MCU, Information and Automation (ICIA), In *2011 IEEE Int. Conf.* 6−8 June 2011; pp 485−489.

(8) Krein, P. T.; Meadows, R. D. The Electroquasistatics of the Capacitive Touch Panel. *IEEE Trans. Ind. Appl.* **1990**, 26 (3), 529−534.

(9) Noda, K.; Tanimura, K. Production of Transparent Conductive Films with Inserted SiO2 Anchor Layer, and Application to a Resistive Touch Panel. *Electron. Commun. Jpn. Part II Electron* **2001**, 84 (7), 39−45.

(10) Ying-Wen, B.; Chang-Yu, C. In Using Serial Resistors to Reduce the Power Consumption of Resistive Touch Panels. *IEEE Int. Symp. on Consumer Electronics*; 20−23 June 2007; pp 1−6.10.1109/ISCE.2007.4382154

(11) Kirchmeyer, S.; Reuter, K. Scientific Importance, Properties and Growing Applications of Poly(3,4-ethylenedioxythiophene). *J. Mater. Chem.* **2005**, 15 (21), 2077−2088.

(12) Xia, Y.; Sun, K.; Ouyang, J. Solution-Processed Metallic Conducting Polymer Films as Transparent Electrode of Optoelectronic Devices. *Adv. Mater.* **2012**, 24 (18), 2436−2440.

(13) Hecht, D. S.; Heintz, A. M.; Lee, R.; Hu, L.; Moore, B.; Cucksey, C.; Risser, S. High Conductivity Transparent Carbon Nanotube Films Deposited from Superacid. *Nanotechnology* **2011**, 22 (7), 075201.

(14) Geng, H.-Z.; Lee, D. S.; Kim, K. K.; Han, G. H.; Park, H. K.; Lee, Y. H. Absorption Spectroscopy of Surfactant-dispersed Carbon Nanotube Film: Modulation of Electronic Structures. *Chem. Phys. Lett.* **2008**, 455 (4−6), 275−278.

(15) Kaempgen, M.; Duesberg, G. S.; Roth, S. Transparent Carbon Nanotube Coatings. *Appl. Surf. Sci.* **2005**, 252 (2), 425−429.

(16) Rowell, M. W.; Topinka, M. A.; McGehee, M. D.; Prall, H.-J.; Dennler, G.; Sariciftci, N. S.; Hu, L.; Gruner, G. Organic Solar Cells with Carbon Nanotube Network Electrodes. *Appl. Phys. Lett.* **2006**, 88 (23), 233506.

(17) Yin, Z.; Sun, S.; Salim, T.; Wu, S.; Huang, X.; He, Q.; Lam, Y. M.; Zhang, H. Organic Photovoltaic Devices Using Highly Flexible Reduced Graphene Oxide Films as Transparent Electrodes. *ACS Nano* **2010**, 4 (9), 5263−5268.

(18) Zheng, Q.; Ip, W. H.; Lin, X.; Yousefi, N.; Yeung, K. K.; Li, Z.; Kim, J.-K. Transparent Conductive Films Consisting of Ultralarge Graphene Sheets Produced by Langmuir−Blodgett Assembly. *ACS Nano* **2011**, 5 (7), 6039−6051.

(19) Eda, G.; Fanchini, G.; Chhowalla, M. Large-area Ultrathin Films of Reduced Graphene Oxide as a Transparent and Flexible Electronic Material. *Nat. Nanotechnol.* **2008**, 3 (5), 270−274.

(20) Rathmell, A. R.; Wiley, B. J. The Synthesis and Coating of Long, Thin Copper Nanowires to Make Flexible, Transparent Conducting Films on Plastic Substrates. *Adv. Mater.* **2011**, *23* (41), 4798−4803.

(21) Scardaci, V.; Coull, R.; Lyons, P. E.; Rickard, D.; Coleman, J. N. Spray Deposition of Highly Transparent, Low-Resistance Networks of Silver Nanowires over Large Areas. *Small* **2011**, *7* (18), 2621−2628.

(22) Hu, L.; Kim, H. S.; Lee, J.-Y.; Peumans, P.; Cui, Y. Scalable Coating and Properties of Transparent, Flexible, Silver Nanowire Electrodes. *ACS Nano* **2010**, *4* (5), 2955−2963.

(23) De, S.; Higgins, T. M.; Lyons, P. E.; Doherty, E. M.; Nirmalraj, P. N.; Blau, W. J.; Boland, J. J.; Coleman, J. N. Silver Nanowire Networks as Flexible, Transparent, Conducting Films: Extremely High DC to Optical Conductivity Ratios. *ACS Nano* **2009**, *3* (7), 1767−1774.

(24) Lee, J.-Y.; Connor, S. T.; Cui, Y.; Peumans, P. Solution-Processed Metal Nanowire Mesh Transparent Electrodes. *Nano Lett.* **2008**, *8* (2), 689−692.

(25) Li, S.; Chen, Y.; Huang, L.; Pan, D. Large-Scale Synthesis of Well-Dispersed Copper Nanowires in an Electric Pressure Cooker and Their Application in Transparent and Conductive Networks. *Inorg. Chem.* **2014**, *53* (9), 4440−4444.

(26) Sachse, C.; Weiß, N.; Gaponik, N.; Müller-Meskamp, L.; Eychmüller, A.; Leo, K. ITO-Free, Small-Molecule Organic Solar Cells on Spray-Coated Copper-Nanowire-Based Transparent Electrodes. *Adv. Energy Mater.* **2014**, *4* (2), 201300737.

(27) The authors are collaborating with Hewlett-Packard to develop transparent conductors for display applications. As part of this collaboration, HP has specified 100 Ohm/square and 90% as the minimum requirements for transparent electrodes.

(28) Hecht, D. S.; Hu, L.; Irvin, G. Emerging Transparent Electrodes Based on Thin Films of Carbon Nanotubes, Graphene, and Metallic Nanostructures. *Adv. Mater.* **2011**, *23* (13), 1482−1513.

(29) Lee, P.; Lee, J.; Lee, H.; Yeo, J.; Hong, S.; Nam, K. H.; Lee, D.; Lee, S. S.; Ko, S. H. Highly Stretchable and Highly Conductive Metal Electrode by Very Long Metal Nanowire Percolation Network. *Adv. Mater.* **2012**, *24* (25), 3326−3332.

(30) U.S. Geological Survey, Mineral Commodity Summaries, Copper. 2011.

(31) Rathmell, A. R.; Bergin, S. M.; Hua, Y.-L.; Li, Z.-Y.; Wiley, B. J. The Growth Mechanism of Copper Nanowires and Their Properties in Flexible, Transparent Conducting Films. *Adv. Mater.* **2010**, *22* (32), 3558−3563.

(32) Zhang, D.; Wang, R.; Wen, M.; Weng, D.; Cui, X.; Sun, J.; Li, H.; Lu, Y. Synthesis of Ultralong Copper Nanowires for High-Performance Transparent Electrodes. *J. Am. Chem. Soc.* **2012**, *134* (35), 14283−14286.

(33) Cui, F.; Yu, Y.; Dou, L.; Sun, J.; Yang, Q.; Schildknecht, C.; Schierle-Arndt, K.; Yang, P. Synthesis of Ultrathin Copper Nanowires Using Tris(trimethylsilyl)silane for High-Performance and Low-Haze Transparent Conductors. *Nano Lett.* **2015**, *15* (11), 7610−7615.

(34) Rathmell, A. R.; Nguyen, M.; Chi, M.; Wiley, B. J. Synthesis of Oxidation-Resistant Cupronickel Nanowires for Transparent Conducting Nanowire Networks. *Nano Lett.* **2012**, *12* (6), 3193−3199.

(35) Wang, X.; Wang, R.; Shi, L.; Sun, J. Synthesis of Metal/Bimetal Nanowires and Their Applications as Flexible Transparent Electrodes. *Small* **2015**, *11* (36), 4737−4744.

(36) Ahn, Y.; Jeong, Y.; Lee, D.; Lee, Y. Copper Nanowire−Graphene Core−Shell Nanostructure for Highly Stable Transparent Conducting Electrodes. *ACS Nano* **2015**, *9* (3), 3125−3133.

(37) Kholmanov, I. N.; Domingues, S. H.; Chou, H.; Wang, X.; Tan, C.; Kim, J.-Y.; Li, H.; Piner, R.; Zarbin, A. J. G.; Ruoff, R. S. Reduced Graphene Oxide/Copper Nanowire Hybrid Films as High-Performance Transparent Electrodes. *ACS Nano* **2013**, *7* (2), 1811−1816.

(38) Chen, Z.; Ye, S.; Stewart, I. E.; Wiley, B. J. Copper Nanowire Networks with Transparent Oxide Shells That Prevent Oxidation without Reducing Transmittance. *ACS Nano* **2014**, *8* (9), 9673−9679.

(39) Im, H.-G.; Jung, S.-H.; Jin, J.; Lee, D.; Lee, J.; Lee, D.; Lee, J.-Y.; Kim, I.-D.; Bae, B.-S. Flexible Transparent Conducting Hybrid Film Using a Surface-Embedded Copper Nanowire Network: A Highly Oxidation-Resistant Copper Nanowire Electrode for Flexible Opto-electronics. *ACS Nano* **2014**, *8* (10), 10973−10979.

(40) Martin Dressel, G. G. *Electrodynamics of Solids: Optical Properties of Electrons in Matter*; Cambridge University Press, 2002.

(41) Wang, W.; Fernando, K. A. S.; Lin, Y.; Meziani, M. J.; Veca, L. M.; Cao, L.; Zhang, P.; Kimani, M. M.; Sun, Y.-P. Metallic Single-Walled Carbon Nanotubes for Conductive Nanocomposites. *J. Am. Chem. Soc.* **2008**, *130* (4), 1415−1419.

(42) Li, X.; Zhu, Y.; Cai, W.; Borysiak, M.; Han, B.; Chen, D.; Piner, R. D.; Colombo, L.; Ruoff, R. S. Transfer of Large-Area Graphene Films for High-Performance Transparent Conductive Electrodes. *Nano Lett.* **2009**, *9* (12), 4359−4363.

(43) Zhu, Y.; Lu, W.; Sun, Z.; Kosynkin, D. V.; Yao, J.; Tour, J. M. High Throughput Preparation of Large Area Transparent Electrodes Using Non-Functionalized Graphene Nanoribbons. *Chem. Mater.* **2011**, *23* (4), 935−939.

(44) Selzer, F.; Weiß; Kneppe, D.; Bormann, L.; Sachse, C.; Gaponik, N.; Eychmuller, A.; Leo, K.; Muller-Meskamp, L. A Spray-coating Process for Highly Conductive Silver Nanowire Networks as the Transparent Top-electrode for Small Molecule Organic Photovoltaics. *Nanoscale* **2015**, *7* (6), 2777−2783.

(45) Ye, E.; Zhang, S.-Y.; Liu, S.; Han, M.-Y. Disproportionation for Growing Copper Nanowires and their Controlled Self-Assembly Facilitated by Ligand Exchange. *Chem. - Eur. J.* **2011**, *17* (11), 3074−3077.

(46) Yang, H.-J.; He, S.-Y.; Tuan, H.-Y. Self-Seeded Growth of Five-Fold Twinned Copper Nanowires: Mechanistic Study, Characterization, and SERS Applications. *Langmuir* **2014**, *30* (2), 602−610.

(47) Ginley, D. S.; Bright, C. Transparent Conducting Oxides. *MRS Bull.* **2000**, *25* (08), 15−18.

(48) Wu, H.; Hu, L.; Rowell, M. W.; Kong, D.; Cha, J. J.; McDonough, J. R.; Zhu, J.; Yang, Y.; McGehee, M. D.; Cui, Y. Electrospun Metal Nanofiber Webs as High-Performance Transparent Electrode. *Nano Lett.* **2010**, *10* (10), 4242−4248.

(49) Atwater, H. A.; Polman, A. Plasmonics for Improved Photovoltaic Devices. *Nat. Mater.* **2010**, *9* (3), 205−213.

(50) Hu, L.; Wu, H.; Cui, Y. Metal Nanogrids, Nanowires, and Nanofibers for Transparent Electrodes. *MRS Bull.* **2011**, *36* (10), 760−765.

(51) Rhodin, T. N. Low Temperature Oxidation of Copper. I. Physical Mechanism1a. *J. Am. Chem. Soc.* **1950**, *72* (11), 5102−5106.

(52) Shi, L.; Wang, R.; Zhai, H.; Liu, Y.; Gao, L.; Sun, J. A Long-term Oxidation Barrier for Copper Nanowires: Graphene Says Yes. *Phys. Chem. Chem. Phys.* **2015**, *17* (6), 4231−4236.

(53) Tenent, R. C.; Barnes, T. M.; Bergeson, J. D.; Ferguson, A. J.; To, B.; Gedvilas, L. M.; Heben, M. J.; Blackburn, J. L. Ultrasmooth, Large-Area, High-Uniformity, Conductive Transparent Single-Walled-Carbon-Nanotube Films for Photovoltaics Produced by Ultrasonic Spraying. *Adv. Mater.* **2009**, *21* (31), 3210−3216.

(54) Kim, T.; Canlier, A.; Kim, G. H.; Choi, J.; Park, M.; Han, S. M. Electrostatic Spray Deposition of Highly Transparent Silver Nanowire Electrode on Flexible Substrate. *ACS Appl. Mater. Interfaces* **2013**, *5* (3), 788−794.

(55) Lee, J. H.; Lee, P.; Lee, D.; Lee, S. S.; Ko, S. H. Large-Scale Synthesis and Characterization of Very Long Silver Nanowires via Successive Multistep Growth. *Cryst. Growth Des.* **2012**, *12* (11), 5598−5605.